Passivity-Based Design of Sliding Modes for Optimal Load Frequency Control

Trip, Sebastian; Cucuzzella, Michele; De Persis, Claudio; van der Schaft, Arjan; Ferrara, Antonella

Published in:
IEEE Transactions on Control Systems Technology

DOI:
10.1109/TCST.2018.2841844

Publication date:
2019

Passivity-Based Design of Sliding Modes for Optimal Load Frequency Control

Sebastian Trip, Michele Cucuzzella, Claudio De Persis, Arjan van der Schaft, and Antonella Ferrara

***Abstract*— This paper proposes a distributed sliding mode (SM) control strategy for *optimal* load frequency control (OLFC) in power networks, where besides frequency regulation, minimization of generation costs is also achieved (economic dispatch). We study a nonlinear power network of interconnected (equivalent) generators, including voltage and second-order turbine-governor dynamics. The turbine-governor dynamics suggest the design of a sliding manifold such that the turbine-governor system enjoys a suitable passivity property, once the sliding manifold is attained. This paper offers a new perspective on OLFC by means of SM control, and in comparison with the existing literature, we relax required dissipation conditions on the generation side and assumptions on the system parameters.**

***Index Terms*— Economic dispatch, incremental passivity, load frequency control (LFC), power systems stability, sliding mode (SM) control.**

I. Introduction

A POWER mismatch between generation and demand gives rise to a frequency in the power network that can deviate from its nominal value. Regulating the frequency back to its nominal value by load frequency control (LFC) is challenging and it is uncertain if current implementations are adequate to deal with an increasing share of renewable energy sources [2]. Traditionally, the LFC is performed at each control area by a primary droop control and a secondary proportional-integral control. To cope with the increasing uncertainties affecting a control area and to improve the controller's performance, advanced control techniques have been proposed to redesign the conventional LFC schemes, such as model predictive control [3], adaptive control [4], fuzzy control [5], and sliding mode (SM) control [6]. However, due to the predefined power flows through the tie lines, the possibility of achieving economically optimal LFC is lost [7]. Besides improving the stability and the dynamic performance of power systems, new control strategies are additionally required to reduce the operational costs of LFC [8]. In this paper, we propose a novel distributed *optimal* LFC (OLFC) scheme that incorporates the economic dispatch into the LFC loop, departing from the conventional tie-line requirements. An up-to-date survey on recent results on offline and online optimal power flows and OLFC can be found in [9]. We restrict ourselves here to a brief overview of online solutions to OLFC that are close to the presented work. Particularly, we focus on distributed solutions, in contrast to more centralized control schemes that have been studied in [10]–[12]. In order to obtain OLFC, the vast majority of distributed solutions appearing in the literature fit in one of two categories. First, the economic dispatch problem is distributively solved by a primal-dual algorithm converging to the solution of the associated Lagrangian dual problem [13]–[24]. This approach generally requires measurements of the loads or the power flows, which is not always desirable in a LFC scheme. This issue is avoided by the second class of solutions, where a distributed consensus algorithm is employed to converge to a state of identical marginal costs, solving the economic dispatch problem in the unconstrained case [25]–[37]. The proposed SM controller design in this paper is compatible with both approaches, although we put the emphasis on a distributed consensus-based solution and remark on the primal-dual-based approach.

A. Main Contributions

SM control has been used to improve the conventional LFC schemes [38], possibly together with disturbance observers [39]. However, the proposed use of SM to obtain a distributed OLFC scheme is new and can offer a few advantages over the previous results on OLFC. Foremost, it is possible to incorporate the widely used second-order model for the turbine-governor dynamics that is generally neglected in the analytical OLFC studies. Since the generated control signals in OLFC schemes adjust continuously and in real time the governor set points, it is important to incorporate the generation side in a satisfactory level of detail. In this paper, we adopt a *nonlinear* model of a power network, including voltage dynamics, having an arbitrarily complex and meshed topology. The generation side is modeled by an equivalent generator including voltage dynamics and second-order turbine-governor dynamics, which is standard in studies

Manuscript received February 28, 2018; accepted May 10, 2018. Date of publication July 19, 2018; date of current version August 6, 2019. Manuscript received in final form May 24, 2018. This work was supported in part by the Netherlands Organization for Scientific Research (NWO) through the research program ENBARK+ under Project 408.urs+.16.005 and in part by the EU Projects MatchIT under Project 82203. Preliminary results have appeared in [1]. Recommended by Associate Editor A. Chakrabortty. *(Corresponding author: Sebastian Trip.)*

S. Trip, M. Cucuzzella, C. De Persis are with ENTEG, Faculty of Science and Engineering, University of Groningen, 9747 AG Groningen, The Netherlands (e-mail: s.trip@rug.nl; m.cucuzzella@rug.nl; c.de.persis@rug.nl).

A. van der Schaft is with the Faculty of Science and Engineering, Johann Bernoulli Institute for Mathematics and Computer Science, University of Groningen, 9747 AG Groningen, The Netherlands (e-mail: a.j.van.der.schaft@rug.nl).

A. Ferrara is with the Dipartimento di Ingegneria Industriale edell'Informazione, University of Pavia, 27100 Pavia, Italy (e-mail: antonella.ferrara@unipv.it).

Color versions of one or more of the figures in this paper are available online at http://ieeexplore.ieee.org.

Digital Object Identifier 10.1109/TCST.2018.2841844

on conventional LFC schemes. We propose a *distributed* SM controller that is shown to achieve frequency control, while minimizing generation costs. The proposed control scheme continuously adjusts the governor set point. Conventional SM controllers can suffer from the notorious drawback known as chattering effect, due to the discontinuous control input. To alleviate this issue, we incorporate the well-known suboptimal second-order SM (SSOSM) control algorithm [40] leading to a continuous control input. To design the controllers obtaining OLFC, we recall an incremental passivity property of the power network [26] that prescribes a suitable sliding manifold. Particularly, the nonpassive turbine-governor system, constrained to this manifold, is shown to be incrementally passive allowing for a passive feedback interconnection, once the closed-loop system evolves on the sliding manifold. The proposed approach differs substantially from two notable exceptions that also incorporate the turbine-governor dynamics ([41], [42]) and shows some benefits. In contrast to [41], we do not impose constraints on the permitted system parameters, and in contrast to [42], we do not impose dissipation assumptions on the generation side and allow for a higher relative degree (see Remark 7). Furthermore, we believe that the chosen approach, where the design of the sliding manifold is inspired by desired passivity properties, offers new perspectives on the control of networks that have similar control objectives as the one presented, e.g., achieving power sharing in microgrids. As this paper is (to the best of our knowledge) the first to use SM control to obtain OLFC, it additionally enables further studies to compare the performance with respect to other approaches found in the literature.

B. Outline

This paper is organized as follows: In Section II, the considered nonlinear model of the power network is introduced, including voltage and second-order turbine-governor dynamics. Particularly, we stress a useful incremental passivity property of the power network model, which we recall in Appendix A. In Section III, we formulate the considered *optimal* LFC (OLFC) problem, which aims besides frequency regulation also for an economic dispatch. In Section IV, we propose a distributed SM controller aiming at OLFC, where we stress that the control signal to the governor is continuous, avoiding chattering. The stability of the power network in closed loop with the distributed SM controller is studied in Section V, exploiting previously established passivity properties. Simulation results are reported and discussed in Section VI, where a small four-area power network is considered. Furthermore, a comparison with another controller suggested in the literature is performed. Finally, some conclusions and possible future research directions are gathered in Section VI.

C. Notation

Let $\mathbf{0}$ be the vector of all zeros of suitable dimension and let $\mathbb{1}_n$ be the vector containing all ones of length n. The ith element of vector x is denoted by x_i. A steady state solution to system $\dot{x} = \zeta(x)$, is denoted by $\overline{x}$, i.e., $\mathbf{0} = \zeta(\overline{x})$. In case the argument of a function is clear from the context, we occasionally write $\zeta(x)$ as ζ. Let $A \in \mathbb{R}^{n\times m}$ be a matrix, then $\mathrm{im}(A)$ is the image of A and $\ker(A)$ is the kernel of A. In case $A \in \mathbb{R}^{n\times n}$ is a positive definite (positive semidefinite) matrix, we write $A \succ 0$ ($A \succeq 0$). The sign function is defined as

$$\mathrm{sgn}(x) := \begin{cases} -1 & \text{if } x < 0 \\ 0 & \text{if } x = 0 \\ 1 & \text{if } x > 0. \end{cases} \tag{1}$$

II. Nonlinear Power Network Model

Throughout this paper, we consider a power network of n interconnected nodes that represent, e.g., (equivalent) generators or control/coherent areas. To make the discussion explicit, we assume that the governing dynamics of the ith node are described by the so-called "single-axis model." However, the upcoming controller design and presented results are expected to be also applicable to different models than the one presented in this section (see Remark 2). Following [43], the considered dynamics of the ith node are[1]

$$\begin{aligned} \dot{\delta}_i &= f_i^b \\ T_{pi}\dot{f}_i^b &= -\left(f_i^b - f^n\right) \\ &\quad + K_{pi}\left(P_{ti} - P_{di} + \sum_{j\in\mathcal{N}_i} V_i V_j B_{ij}\sin\left(\delta_i - \delta_j\right)\right) \qquad (2) \\ T_{Vi}\dot{V}_i &= \overline{E}_{fi} - \left(1 - (X_{di} - X'_{di})B_{ii}\right)V_i \\ &\quad - \left(X_{di} - X'_{di}\right)\sum_{j\in\mathcal{N}_i} V_j B_{ij}\cos\left(\delta_i - \delta_j\right) \qquad (3) \end{aligned}$$

where $\mathcal{N}_i$ is the set of nodes connected to the ith node by transmission lines. We assume that the network is lossless, which is generally valid in high-voltage transmission networks where the line resistance is negligible. The voltage V generally corresponds to the q-axis internal voltage and we do not differentiate between the generator internal and terminal buses. Moreover, P_{ti} in (3) is the power generated by the ith (equivalent) plant and can be expressed as the output of the following second-order dynamical system that describes the behavior of both the governor and the turbine

$$\begin{aligned} T_{ti}\dot{P}_{ti} &= -P_{ti} + P_{gi} \\ T_{gi}\dot{P}_{gi} &= -\frac{1}{R_i}\left(f_i^b - f^n\right) - P_{gi} + u_i. \end{aligned} \tag{4}$$

The symbols used in (3) and (4) are described in Table I. To further illustrate the dynamics, a block diagram for a two generator network is provided in Fig 1. In this paper, we aim at the design of a continuous control input u_i to achieve both the frequency regulation and economic efficiency (OLFC).

The network topology is represented by a connected and undirected graph $\mathcal{G} = (\mathcal{V}, \mathcal{E})$, where $\mathcal{V} = \{1, \ldots, n\}$ is the set of nodes and $\mathcal{E} = \{1, \ldots, m\}$ is the set of edges, representing the transmission lines connecting the nodes. The topology can be described by its corresponding incidence matrix $\mathcal{B} \in \mathbb{R}^{n\times m}$.

[1]For notational simplicity, the dependence of the variables on time t is mostly omitted throughout this paper

TABLE I
DESCRIPTION OF THE USED SYMBOLS

	State variables
δ_i	Voltage angle
f_i^b	Frequency
f_i	Frequency deviation
V_i	Voltage
P_{ti}	Turbine output power
P_{gi}	Governor output
	Parameters
f^n	Nominal frequency
T_{pi}	Time constant of the generator
T_{ti}	Time constant of the turbine
T_{gi}	Time constant of the governor
T_{Vi}	Direct axis transient open-circuit constant
K_{pi}	Gain of the generator
R_i	Speed regulation coefficient
X_{di}	Direct synchronous reactance
X'_{di}	Direct synchronous transient reactance
B_{ij}	Transmission line susceptance
	Inputs
u_i	Control input to the governor
$\overline{E}_{fi}$	Constant exciter voltage
P_{di}	Unknown power demand

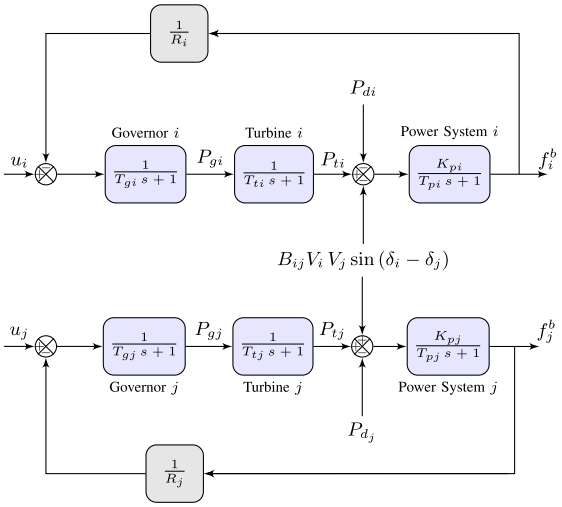

Fig. 1. Block diagram of two interconnected generators. The voltage dynamics are omitted.

Then, by arbitrarily labeling the ends of edge k with a $+$ and a $-$, one has that

$$\mathcal{B}_{ik} = \begin{cases} +1 & \text{if } i \text{ is the positive end of } k \\ -1 & \text{if } i \text{ is the negative end of } k \\ 0 & \text{otherwise.} \end{cases}$$

To study the power network, we write system (3) compactly for all nodes $i \in \mathcal{V}$ as

$$\begin{aligned} \dot{\eta} &= \mathcal{B}^T f \\ T_p \dot{f} &= -f + K_p(P_t - P_d - \mathcal{B}\Gamma(V)\sin(\eta)) \\ T_V \dot{V} &= -\big(X_d - X'_d\big)E(\eta)V + \overline{E}_f \end{aligned} \tag{5}$$

and the turbine-governor dynamics in (4) as

$$\begin{aligned} T_t \dot{P}_t &= -P_t + P_g \\ T_g \dot{P}_g &= -R^{-1} f - P_g + u \end{aligned} \tag{6}$$

where $f = f^b - f^n \mathbb{1}_n \in \mathbb{R}^n$ is the frequency deviation, $\eta = \mathcal{B}^T \delta \in \mathbb{R}^m$ is the vector describing the differences in voltage angles. Furthermore, $\Gamma = \text{diag}\{\Gamma_1, \ldots, \Gamma_m\}$, where $\Gamma(V)_k = V_i V_j B_{ij}$, with $k \sim \{i, j\}$, i.e., line k connects nodes i and j. The components of the matrix $E(\eta) \in \mathbb{R}^{n \times n}$ are defined as

$$\begin{aligned} E_{ii}(\eta) &= \frac{1}{X_{di} - X'_{di}} - B_{ii} \quad i \in \mathcal{V} \\ E_{ij}(\eta) &= B_{ij}\cos(\eta_k) = E_{ji}(\eta) \quad k \sim \{i, j\} \in \mathcal{E} \\ E_{ij}(\eta) &= 0 \quad \text{otherwise.} \end{aligned} \tag{7}$$

The remaining symbols follow straightforwardly from (3) and (4), and are the vectors and matrices of suitable dimensions.

In the remainder of this paper, we assume that there exists a (suitable) steady state solution to the power network model (5) and (6).

Assumption 1 (Steady State Solution): The unknown power demand (unmatched disturbance) P_d is constant and for a given $\overline{P}_t$, there exist a $\overline{u}$ and state $(\overline{\eta}, \overline{f}, \overline{V}, \overline{P}_t, \overline{P}_g)$ that satisfies

$$\begin{aligned} \mathbf{0} &= \mathcal{B}^T \overline{f} \\ \mathbf{0} &= -\overline{f} + K_p(\overline{P}_t - P_d - \mathcal{B}\Gamma(\overline{V})\ \sin(\overline{\eta})) \\ \mathbf{0} &= -\big(X_d - X'_d\big)E(\overline{\eta})\overline{V} + \overline{E}_f \end{aligned} \tag{8}$$

and

$$\begin{aligned} \mathbf{0} &= -\overline{P}_t + \overline{P}_g \\ \mathbf{0} &= -R^{-1}\overline{f} - \overline{P}_g + \overline{u}. \end{aligned} \tag{9}$$

◇

An important property of system (5) is that is incrementally (cyclo) passive (see Definition 1 in Appendix A) with respect to a steady state solution $(\overline{\eta}, \overline{f}, \overline{V}, \overline{P}_t, \overline{P}_g)$ satisfying (8) and (9). This has been established before in [26], and we recall the most important results in Appendix A at the end of this paper.

Remark 1 (Reactance and Susceptance): For each (equivalent) generator $i \in \mathcal{V}$, the reactance is higher than the transient reactance, i.e., $X_{di} > X'_{di}$ [44]. Furthermore, the self-susceptance of node $i \in \mathcal{V}$ is given by $B_{ii} = \sum_{j \in \mathcal{N}_i} B_{ij}$ and the susceptance of a line satisfies $B_{ij} = B_{ji} < 0$. Consequently, $E(\eta)$ is a strictly diagonally dominant and symmetric matrix with positive elements on its diagonal and is therefore positive definite. ◇

Remark 2 (Incremental Passivity and Applicability to Other Power Network Models): The focus of this paper is to achieve OLFC by distributed SM control for a nonlinear power network, explicitly taking into account the turbine-governor dynamics. Equation (5) is often adequately enough to represent a power network for the purpose of frequency regulation and are often further simplified by assuming constant voltages, leading to the so-called "swing equations." To the controller

design and the analysis in this paper, an incremental passivity property that is established in Appendix A is essential. This property has been established for various other models, including structure-preserving high voltage networks [41] or networks including sixth-order generator models [45]. Furthermore, underlying energy functions have been established for networks including internal and terminal generator buses and dynamic load models [46], [47]. It is therefore expected that the presented approach can straightforwardly be applied to a wider range of models than the one we consider in this paper. ◇

III. Optimal Frequency Regulation

We continue this paper by formulating the control objectives of OLFC. Before doing so, we first note that the steady-state frequency $\overline{f}$, is generally different from zero without proper adjustments of the input $\overline{u}$ [26].

Lemma 1 (Steady-State Frequency): Let Assumption 1 hold, then necessarily $\overline{f} = \mathbb{1}_n f^*$ with

$$f^* = \frac{\mathbb{1}_n^T(\overline{u} - P_d)}{\mathbb{1}_n^T\left(K_p^{-1} + R^{-1}\right)\mathbb{1}_n} \tag{10}$$

where $\mathbb{1}_n \in \mathbb{R}^n$ is the vector consisting of all ones. ◇

This leads us to the first objective, concerning the regulation of the frequency deviation.

Objective 1 (Frequency Regulation): The frequency deviation f asymptotically converges to zero, that is,

$$\lim_{t\to\infty} f(t) = \mathbf{0}. \tag{11}$$

◇

From (10), it is clear that it is sufficient that $\mathbb{1}_n^T(\overline{u} - P_d) = 0$, to have zero frequency deviation at the steady state. Therefore, there is a flexibility to distribute the total required generation optimally among the various (equivalent) generators. To make the notion of optimality explicit, we assign to every generator a strictly convex linear-quadratic cost function $C_i(P_{ti})$ related to the generated power P_{ti}

$$C_i(P_{ti}) = \frac{1}{2}\mathcal{Q}_i P_{ti}^2 + \mathcal{R}_i P_{ti} + \mathcal{C}_i \quad \forall i \in \mathcal{V}. \tag{12}$$

Minimizing the total generation cost, subject to the constraint that allows for a zero frequency deviation can then be formulated as the following optimization problem:

$$\begin{aligned} \min \quad & \sum_{i\in\mathcal{V}} C_i(P_{ti}) \\ \text{s.t.} \quad & \mathbb{1}_n^T(\overline{u} - P_d) = 0. \end{aligned} \tag{13}$$

Note that the above-mentioned optimization problem is convex, since no additional (tie line) constraints on the power flows are considered. Indeed, it is common for OLFC schemes to replace the line constraints in favor of an online economic dispatch of the generators. In case the resulting power flows are close to the line limits, feasibility of resulting steady-state power flows can be guaranteed by relying, e.g., on a primal-dual-based approach (see Remark 8), where additional line constraint can be incorporated within the optimization problem (13) [15]. The lemma below makes the solution to (13) explicit [26]:

Lemma 2 (Optimal Generation): The solution $\overline{P}_t^{\text{opt}}$ to (13) satisfies

$$\overline{P}_t^{\text{opt}} = \mathcal{Q}^{-1}(\overline{\lambda}^{\text{opt}} - \mathcal{R}) \tag{14}$$

where

$$\overline{\lambda}^{\text{opt}} = \frac{\mathbb{1}_n\mathbb{1}_n^T(P_d + \mathcal{Q}^{-1}\mathcal{R})}{\mathbb{1}_n^T\mathcal{Q}^{-1}\mathbb{1}_n} \tag{15}$$

and $\mathcal{Q} = \text{diag}(\mathcal{Q}_1, \ldots, \mathcal{Q}_n)$, $\mathcal{R} = (\mathcal{R}_1, \ldots, \mathcal{R}_n)^T$. ◇

From (14), it follows that the marginal costs $\mathcal{Q}\overline{P}_t^{opt} + \mathcal{R}$ are identical. Note that (14) depends explicitly on the *unknown* power demand P_d. We aim at the design of a controller solving (13) without measurements of the power demand, leading to the second objective.

Objective 2 (Economic Dispatch): The generated power P_t asymptotically converges to the optimal power generation, that is,

$$\lim_{t\to\infty} P_t(t) = \overline{P}_t^{\text{opt}} \tag{16}$$

with $\overline{P}_t^{\text{opt}}$ as in (14). ◇

In order to achieve Objective 1 and Objective 2, we refine Assumption 1 that ensures the feasibility of the objectives.

Assumption 2 (Existence of an Optimal Steady State): Assumption 1 holds when $\overline{f} = \mathbf{0}$ and $\overline{P}_t = \overline{P}_g = \overline{P}_t^{\text{opt}}$, with $\overline{P}_t^{\text{opt}}$ as in (14). ◇

IV. Distributed Sliding Mode Control

In this section, we propose a distributed SM controller to achieve Objective 1 and Objective 2 for the power network (5). To facilitate the upcoming discussion, a few essential definitions of SM control are gathered in Appendix B. Furthermore, in order to permit the controller design, the following assumption is made on the *unknown* demand (unmatched disturbance) and the available measurements:

Assumption 3 (Available Information): The variables f_i, P_{ti}, and P_{gi} are locally available[2] at node i. All the network parameters and the power demand P_d are constant and unknown, but with known bounds. ◇

In Appendix A, a passivity property of the power network (5) is recalled, with input P_t and output f. Unfortunately, the turbine-governor system (6) does not immediately allow for a passive interconnection, since (6) is a linear system with relative degree two, when considering $-f$ as the input and P_t as the output.[3] This makes the controller design more challenging and is a major reason why the turbine-governor dynamics are generally neglected or approximated by a first-order system in analytical OLFC studies. To alleviate this issue, we propose a *distributed* SSOSM (D-SSOSM) control algorithm that simultaneously achieves Objective 1 and Objective 2, by constraining (6) such that it enjoys a

[2]In case not all variables are locally available, Assumption 3 can be relaxed by implementing observers that estimate the unmeasured states in a finite time (see for instance [48]).

[3]A linear system with relative degree two is not passive, as follows, e.g., from the Kalman–Yakubovich–Popov lemma.

suitable passivity property, and by exchanging information on the marginal costs. As a first step (see Remark 3), we augment the turbine-governor dynamics (6) with a distributed control scheme, resulting in

$$\begin{aligned} T_t \dot{P}_t &= -P_t + P_g \\ T_g \dot{P}_g &= -R^{-1} f - P_g + u \\ T_\theta \dot{\theta} &= -\theta + P_t - A\mathcal{L}^{\text{com}}(\mathcal{Q}\theta + \mathcal{R}). \end{aligned} \tag{17}$$

Here, $\mathcal{Q}\theta + \mathcal{R}$ reflects the "virtual" marginal costs and $\mathcal{L}^{\text{com}}$ is the Laplacian matrix corresponding to the topology of an underlying communication network. The diagonal matrix $T_\theta \in \mathbb{R}^{n\times n}$ provides the additional design freedom to shape the transient response and the matrix A is suggested later to obtain a suitable passivity property. We note that $\mathcal{L}^{\text{com}}(\mathcal{Q}\theta + \mathcal{R})$ represents the exchange of information on the marginal costs among the nodes. To guarantee an optimal coordination of generation among *all* the nodes the following assumption is made:

Assumption 4 (Communication Topology): The graph corresponding to the communication topology is balanced and strongly connected.[4] ◇

We now propose a sliding function $\sigma(f, P_t, P_g, \theta)$ and a matrix A for system (17), which will allow us to prove convergence to the desired state. The choices are motivated by the stability analysis in Section V, but are stated here for the sake of exposition. First, the sliding function $\sigma : \mathbb{R}^{4n} \to \mathbb{R}^n$ is given as

$$\sigma(f, P_t, P_g, \theta) = M_1 f + M_2 P_t + M_3 P_g + M_4 \theta \tag{18}$$

where $M_1 \succ 0$, $M_2 \succeq 0$, $M_3 \succ 0$ are the diagonal matrices and $M_4 = -(M_2 + M_3)$. Therefore, $\sigma_i, i \in \mathcal{V}$, depends only on the locally available variables that are defined on node i, facilitating the design of a distributed controller (see Remark 5). Second, the diagonal matrix $A \in \mathbb{R}^{n\times n}$ is defined as

$$A = (M_2 + M_3)^{-1} M_1 \mathcal{Q}. \tag{19}$$

By regarding the sliding function (18) as the output function of system (5), (17), it appears that the relative degree of the system is one. This implies that a first-order SM controller can be *naturally* applied [49] to attain in a finite time, the sliding manifold defined by $\sigma = \mathbf{0}$. However, the input u to the governor affects the first time derivative of the sliding function, i.e., u affects $\dot{\sigma}$. Since SM controllers generate a discontinuous signal, we additionally require $\dot{\sigma} = \mathbf{0}$, to guarantee that the signal u is continuous. Therefore, we define the desired sliding manifold as

$$\{(\eta, f, V, P_t, P_g, \theta) : \sigma = \dot{\sigma} = \mathbf{0}\}. \tag{20}$$

We continue in Section IV-A with discussing a possible controller attaining the desired sliding manifold (20) while providing a continuous control input u.

[4]A directed graph is balanced if the (weighted) in-degree is equal to the (weighted) out-degree of every node and it is strongly connected if there is a directed path from any node to every other node. A balanced and strongly connected graph implies that $\mathcal{L}^{\text{com}} + (\mathcal{L}^{\text{com}})^T = \hat{\mathcal{L}}^{\text{com}} \succeq 0$ and that $\ker(\hat{\mathcal{L}}^{\text{com}}) = \text{im}(\mathbb{1}_n)$. Any undirected and connected graphs are balanced and strongly connected.

Remark 3 (First-Order Turbine-Governor Dynamics): The rationale behind this seemingly *ad hoc* choice of the augmented dynamics is that for the controlled first-order turbine-governor dynamics, where $u = \theta$ and $P_g = -R^{-1} f + \theta$, system

$$\begin{aligned} T_t \dot{P}_t &= -P_t - R^{-1} f + \theta \\ T_\theta \dot{\theta} &= -\theta + P_t - R^{-1}\mathcal{Q}\mathcal{L}^{\text{com}}(\mathcal{Q}\theta + \mathcal{R}) \end{aligned} \tag{21}$$

has been shown to be incrementally passive with the input $-f$ and output P_t, and is able to solve Objective 1 and Objective 2 [41]. We aim at the design of u and A in (17), such that (17) behaves similarly as (21). This is made explicit in Lemma 4. ◇

A. Suboptimal Second-Order Sliding Mode Controller

To prevent chattering, it is important to provide a continuous control input u to the governor. Since SM controllers generate a discontinuous control signal, we adopt the procedure suggested in [40] and first integrate the discontinuous signal, yielding for system (17)

$$\begin{aligned} T_t \dot{P}_t &= -P_t + P_g \\ T_g \dot{P}_g &= -R^{-1} f - P_g + u \\ T_\theta \dot{\theta} &= -\theta + P_t - A\mathcal{L}^{\text{com}}(\mathcal{Q}\theta + \mathcal{R})\dot{u} = w \end{aligned} \tag{22}$$

where w is the new (discontinuous) input generated by a SM controller discussed as follows. A consequence is that the system relative degree (with respect to the new control input w) is now two, and we need to rely on a second-order SM control strategy to attain the sliding manifold (18) in a finite time [50]. To make the controller design explicit, we discuss a specific second-order SM controller, the so-called SSOSM controller proposed in [40]. We introduce two auxiliary variables $\xi_1 = \sigma \in \mathbb{R}^n$ and $\xi_2 = \dot{\sigma} \in \mathbb{R}^n$, and define the so-called auxiliary system as

$$\begin{aligned} \dot{\xi}_1 &= \xi_2 \\ \dot{\xi}_2 &= \phi(\eta, f, V, P_t, P_g, \theta) + Gw. \end{aligned} \tag{23}$$

Bearing in mind that $\dot{\xi}_2 = \ddot{\sigma} = \phi + Gw$, the expressions for the mapping ϕ and matrix G can straightforwardly be obtained from (18) by taking the second derivative of σ with respect to time, yielding for the latter[5] $G = M_3 T_g^{-1} \in \mathbb{R}^{n\times n}$. We assume that the entries of ϕ and G have known bounds

$$|\phi_i| \le \Phi_i \quad \forall\, i \in \mathcal{V} \tag{24}$$

$$0 < G_{\min_i} \le G_{ii} \le G_{\max_i} \quad \forall\, i \in \mathcal{V} \tag{25}$$

with Φ_i, $G_{\min_i}$, and $G_{\max_i}$ being the positive constants. Second, w is a discontinuous control input described by the SSOSM control algorithm [40], and consequently for each node $i \in \mathcal{V}$, the control law w_i is given as

$$w_i = -\alpha_i W_{\max_i} \operatorname{sgn}\left(\xi_{1_i} - \frac{1}{2}\xi_{1,\max_i}\right) \tag{26}$$

with

$$W_{\max_i} > \max\left(\frac{\Phi_i}{\alpha_i^* G_{\min_i}}; \frac{4\Phi_i}{3G_{\min_i} - \alpha_i^* G_{\max_i}}\right) \tag{27}$$

[5]The expression for ϕ is rather long and is omitted.

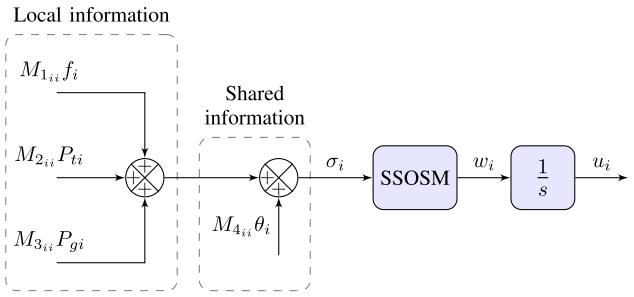

Fig. 2. Block diagram of the proposed D-SSOSM control strategy.

$$\alpha_i^* \in (0, 1] \cap \left(0, \frac{3G_{\min_i}}{G_{\max_i}}\right) \tag{28}$$

α_i switching between α_i^* and 1, according to [40, Algorithm 1]. Note that indeed the input signal to the governor, $u(t) = \int_0^t w(\tau)d\tau$, is continuous, since the input w is the piecewise constant. The extremal values $\xi_{1,\max_i}$ in (26) can be detected by implementing for instance a peak detection as in [51]. The block diagram of the proposed control strategy is depicted in Fig 2.

Remark 4 (Uncertainty of ϕ and G): The mapping ϕ and matrix G are uncertain due to the presence of the unmeasurable power demand P_d and voltage angle θ, and possible uncertainties in the system parameters. In practical cases, the bounds in (24) and (25) can be determined relying on data analysis and physical insights. However, if these bounds cannot be *a priori* estimated, the adaptive version of the SSOSM algorithm proposed in [52] can be used to dominate the effect of the uncertainties. ◇

Remark 5 (Distributed Control): Given A in (19), the dynamics of θ_i in (17) read for node $i \in \mathcal{V}$ as

$$T_{\theta i}\dot{\theta}_i = -\theta_i + P_{ti} - \frac{\mathcal{Q}_i M_{1_{ii}}}{M_{2_{ii}} + M_{3_{ii}}} \sum_{j \in \mathcal{N}_i^{\text{com}}} (\mathcal{Q}_i\theta_i + \mathcal{R}_i - \mathcal{Q}_j\theta_j - \mathcal{R}_j)$$

where $\mathcal{N}_i^{\text{com}}$ is the set of controllers connected to controller i. Furthermore, (26) depends only on σ_i, i.e., on states defined at node i. Consequently, the overall controller is indeed distributed and only information on marginal costs needs to be shared among the connected controllers. ◇

Remark 6 (Alternative SOSM Controllers): In this paper, we rely on the SOSM control law proposed in [40]. However, to constrain system (5) augmented with dynamics (22) on the sliding manifold (20), where $\sigma = \dot{\sigma} = \mathbf{0}$, any other SOSM control law that does not need the measurement of $\dot{\sigma}$ can be used, e.g., the super-twisting control [53]. An interesting continuation of the presented results is to study the performance of various SOSM controllers within the setting of (optimal) LFC. ◇

Remark 7 (Comparison With [41] and [42]): The controller proposed in [41] requires, besides a gain restriction in the controller, that

$$\begin{aligned} 4T_{gi}T_{ti}^{-1} &> 1 \\ K_{pi}^{-1}T_{gi}T_{ti}^{-1} &> 1. \end{aligned} \tag{29}$$

In this paper, we do not impose such restriction on the parameters. The result in [42] requires, besides some assumptions on the dissipation inequality related to the generation side, the existence of frequency-dependent generation and load, where the generation/demand (output) depends directly (e.g., proportionally) on the frequency (input), avoiding complications arising from generation dynamics that have relative degree two when considering the input–output pair just indicated (see Remark 9). ◇

Remark 8 (Primal-Dual-Based Approaches): Although the focus in this paper is to augment the power network with consensus-type dynamics in (17), it is equally possible to augment the power network with a continuous primal-dual algorithm that has been studied extensively to obtain optimal LFC. This paper, therefore, also provides means to extend existing results on primal-dual-based approaches to incorporate the turbine-governor dynamics, generating the control input by a higher order SM controller. The required adjustments follow similar steps as discussed in [41, Remark 9], and for the sake of brevity, we directly state the resulting primal-dual-based augmented system, replacing (17)

$$\begin{aligned} T_t\dot{P}_t &= -P_t + P_g \\ T_g\dot{P}_g &= -R^{-1}f - P_g + u \\ T_\theta\dot{\theta} &= -\theta + P_t - M_1(M_2 + M_3)^{-1}(\nabla C(\theta) - \lambda) \\ \dot{\upsilon} &= -\mathcal{B}^T\lambda \\ \dot{\lambda} &= \mathcal{B}\upsilon - \theta + P_d. \end{aligned} \tag{30}$$

In this case only strict convexity of $C(\cdot)$ is required and the load P_d explicitly appears in (30). The stability analysis of the power network, including the augmented turbine-governor dynamics (30), follows *mutatis mutandis*, the same argumentation as in the next section where the focus is on the augmented system (17). Some required nontrivial modifications in the analysis are briefly discussed in Remark 13. ◇

V. Stability Analysis and Main Result

In this section, we study the stability of the proposed control scheme, based on an enforced passivity property of (17) on the sliding manifold defined by (18). First, we establish that the second-order SM controller (23)–(28) constrains the system in finite time to the desired sliding manifold.

Lemma 3 (Convergence to the Sliding Manifold): Let Assumption 3 hold. The solutions to system (5), augmented with (22), in closed loop with controller (23)–(28) converge in a finite time T_r to the sliding manifold (20) such that

$$P_g = -M_3^{-1}(M_1 f + M_2 P_t + M_4\theta) \quad \forall\, t \geq T_r. \tag{31}$$

Proof: Following [40], the application of (23)–(28) to each (equivalent) generator guarantees that $\sigma = \dot{\sigma} = \mathbf{0}$, $\forall t \geq T_r$. The details are omitted, and are an immediate consequence of the used SSOSM control algorithm [40]. Then, from (18) one can easily obtain (31), where M_3 is the indeed invertible. ■

Exploiting relation (31), on the sliding manifold where $\sigma = \dot{\sigma} = \mathbf{0}$, the so-called equivalent system is as

follows:

$$M_3 T_t \dot{P}_t = -(M_2 + M_3)P_t - M_4\theta - M_1\ f$$
$$T_\theta \dot{\theta} = -\theta + P_t - A\mathcal{L}^{\text{com}}(\mathcal{Q}\theta + \mathcal{R}). \quad (32)$$

As a consequence of the feasibility assumption (Assumption 1), the system above admits the following steady state:

$$\mathbf{0} = -(M_2 + M_3)\overline{P}_t^{\text{opt}} - M_4\overline{\theta} - M_1\mathbf{0}$$
$$\mathbf{0} = -\overline{\theta} + \overline{P}_t^{\text{opt}} - A\mathcal{L}^{\text{com}}(\mathcal{Q}\overline{\theta} + \mathcal{R}). \quad (33)$$

Now, we show that system (32), with A as in (19), indeed possesses a passivity property with respect to the steady state (33). Note that, due to the discontinuous control law (26), the solutions to the closed-loop system are understood in the sense of Filippov. Following the equivalent control method [49], the solutions to the equivalent system are, however, continuously differentiable.

Lemma 4 (Incremental Passivity of (32)): System (32) with input $-f$ and output P_t is an incrementally passive system, with respect to the constant $(\overline{P}_t^{\text{opt}}, \overline{\theta})$ satisfying (33).

Proof: Consider the following incremental storage function:

$$\mathcal{S}_2 = \frac{1}{2}\big(P_t - \overline{P}_t^{\text{opt}}\big)^T M_1^{-1} M_3 T_t \big(P_t - \overline{P}_t^{\text{opt}}\big) + \frac{1}{2}(\theta - \overline{\theta})^T M_1^{-1}(M_2 + M_3)T_\theta(\theta - \overline{\theta}) \quad (34)$$

which is the positive definite, since $M_1 \succ 0, M_2 \succeq 0$ and $M_3 \succ 0$. Then, we have that $\mathcal{S}_2$ satisfies along the solutions to (32)

$$\begin{aligned}\dot{\mathcal{S}}_2 &= \big(P_t - \overline{P}_t^{\text{opt}}\big)^T M_1^{-1} M_3\ T_t \dot{P}_t \\ &\quad + (\theta - \overline{\theta})^T M_1^{-1}(M_2 + M_3)T_\theta \dot{\theta}, \\ &= \big(P_t - \overline{P}_t^{\text{opt}}\big)^T (-M_1^{-1}(M_2 + M_3)P_t - f - M_1^{-1}M_4\theta) \\ &\quad + (\theta - \overline{\theta})^T M_1^{-1}(M_2 + M_3)\cdot\big(P_t - \theta - A\mathcal{L}^{\text{com}}(\mathcal{Q}\theta + \mathcal{R})\big).\end{aligned}$$

In view of $M_4 = -(M_2 + M_3)$, $A = (M_2 + M_3)^{-1}M_1\mathcal{Q}$ and equality (33), it follows that:

$$\begin{aligned}\dot{\mathcal{S}}_2 &= -(P_t - \theta)^T M_1^{-1}(M_2 + M_3)(P_t - \theta) \\ &\quad -(\mathcal{Q}\theta + \mathcal{R} - \mathcal{Q}\overline{\theta} - R)\hat{\mathcal{L}}^{\text{com}}(\mathcal{Q}\theta + \mathcal{R} - \mathcal{Q}\overline{\theta} - \mathcal{R}) \\ &\quad -\big(P_t - \overline{P}_t^{\text{opt}}\big)^T (f - \mathbf{0})\end{aligned}$$

where $\hat{\mathcal{L}}^{\text{com}} = \frac{1}{2}(\mathcal{L}^{\text{com}} + (\mathcal{L}^{\text{com}})^T) \succeq 0$ (see Assumption 4). ■

Relying on the interconnection of incrementally passive systems, we can prove the main result of this paper concerning the evolution of the augmented system controlled via the proposed distributed SSOSM control strategy. Note that the proof exploits the incremental passivity property of the power network (5), which is derived in Appendix A.

Theorem 1 (Main Result: Distributed OLFC): Let Assumptions 1–6 hold. Consider the systems (5) and (17), controlled via (23)–(28). Then, the solutions to the closed-loop system starting in a neighborhood of the equilibrium $(\overline{\eta}, \overline{f} = \mathbf{0}, \overline{V}, \overline{P}_t^{\text{opt}}, \overline{P}_g, \overline{\theta})$ approach the set where $\overline{f} = \mathbf{0}$ and $\overline{P}_t = \overline{P}_t^{\text{opt}}$, with $\overline{P}_t^{\text{opt}}$ given by (14).

Proof: Following Lemma 3, we have that the SSOSM control enforces system (17) to evolve $\forall\, t \geq T_r$ on the sliding manifold (20), resulting in the reduced order system (32). To study the obtained closed-loop system, consider the overall incremental storage function $\mathcal{S} = \mathcal{S}_1 + \mathcal{S}_2$, with $\mathcal{S}_1$ given by (44) and $\mathcal{S}_2$ given by (34). In view of Lemma 6, we have that $\mathcal{S}$ has a local minimum at $(\overline{\eta}, \overline{f} = \mathbf{0}, \overline{V},\ \overline{P}_t^{\text{opt}}, \overline{\theta})$ and satisfies (see Lemma 4 and Lemma 5) along the solutions to (5) and (32)

$$\begin{aligned}\dot{\mathcal{S}} &= -f^T K_p^{-1} f - \dot{V}^T T_V \big(X_d - X_d'\big)^{-1}\dot{V} \\ &\quad -(P_t - \theta)^T M_1^{-1}(M_2 + M_3)(P_t - \theta) \\ &\quad -(\mathcal{Q}\theta + \mathcal{R} - \mathcal{Q}\overline{\theta} - R)\hat{\mathcal{L}}^{\text{com}}(\mathcal{Q}\theta + \mathcal{R} - \mathcal{Q}\overline{\theta} - \mathcal{R}) \\ &\leq 0\end{aligned}$$

where $\dot{V} = T_V^{-1}(-(X_d - X_d')E(\eta)V + \overline{E}_f)$. Consequently, there exists a forward invariant set Υ around $(\overline{\eta}, \overline{f} = \mathbf{0}, \overline{V},\ \overline{P}_t^{\text{opt}}, \overline{\theta})$ and by LaSalle's invariance principle the solutions that start in Υ approach the largest invariant set contained in

$$\Upsilon \cap \{(\eta, f, V,\ P_t, \theta) : f = \mathbf{0}, V = \big((X_d - X_d')E(\overline{\eta})\big)^{-1}\overline{E}_f \\ P_t = \theta, \theta = \overline{\theta} + \mathcal{Q}^{-1}\mathbb{1}\alpha\} \quad (35)$$

where $\alpha \in \mathbb{R}$ is some scalar. On this invariant set the controlled power network satisfies

$$\begin{aligned}\dot{\eta} &= \mathcal{B}^T\mathbf{0} \\ \mathbf{0} &= K_p(\overline{\theta} + \mathcal{Q}^{-1}\mathbb{1}\alpha - P_d - \mathcal{B}\Gamma(V)\sin(\eta)) \\ \mathbf{0} &= -\big(X_d - X_d'\big)E(\eta)V + \overline{E}_f \\ M_3 T_t \dot{P}_t &= \mathbf{0} \\ T_\theta \dot{\theta} &= \mathbf{0}. \quad (36)\end{aligned}$$

Premultiplying both sides of the second line of (36) with $\mathbb{1}_n^T K_p^{-1}$ yields $0 = \mathbb{1}_n^T(\overline{\theta} + \mathcal{Q}^{-1}\mathbb{1}\alpha - P_d)$. Since $\overline{\theta} = \overline{P}_t^{\text{opt}}$, $\mathbb{1}_n^T(\overline{P}_t^{\text{opt}} - P_d) = 0$ and $\mathcal{Q}$ is a diagonal matrix with only positive elements, it follows that necessarily $\alpha = 0$. We can conclude that the solutions to the system (5) and (17), controlled via (23)–(28), indeed approach the set where $\overline{f} = \mathbf{0}$ and $\overline{P}_t = \overline{P}_t^{\text{opt}}$, with $\overline{P}_t^{\text{opt}}$ given by (14). Furthermore, from (31) it follows that also P_g approaches the set where $P_g = P_t = \overline{P}_t^{\text{opt}}$. ■

Remark 9 (Reducing the Relative Degree): An important consequence of the proposed SM controller (23)–(28) is that the relative degree of system (32) is one with input $-f$ and output P_t. This is in contrast to the "original" system (6) that has relative degree two with the same input–output pair. ◇

Remark 10 (Varying Power Demand): To allow for a steady state solution, the power demand (unmatched disturbance) is required to be constant. This is not needed to reach the desired sliding manifold, but is required only to establish the asymptotic convergence properties in Objective 1 and Objective 2. Furthermore, the proposed solution shows ([26, Remark 8]) the existence of a finite $\mathcal{L}_2$-to-$\mathcal{L}_\infty$ gain and a finite $\mathcal{L}_2$-to-$\mathcal{L}_2$ gain from a varying demand to the frequency deviation f [54], once the system evolves on the sliding manifold. ◇

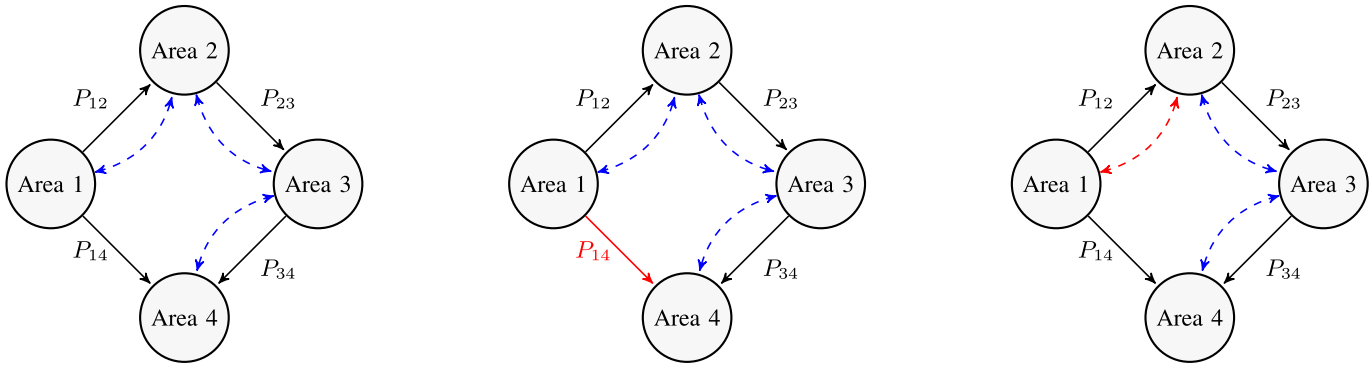

Fig. 3. Scheme of the considered power network partitioned into four areas, where $P_{ij} = (V_i V_j / X_{ij}) \sin(\delta_i - \delta_j)$. Solid arrows: positive direction of the power flows through the power network. Dashed lines: communication network. From the left, the configurations of the considered scenarios are represented, where the components that are failing/removed during the simulation are colored red.

Remark 11 (Robustness to Failed Communication): The proposed control scheme is distributed and as such requires a communication network to share information on the marginal costs. However, note that the term $-A\mathcal{L}^{\text{com}}(\mathcal{Q}\theta + \mathcal{R})$ in (17) is not needed to enforce the passivity property established in Lemma 4, but is required to prove convergence to the economic efficient generation $\overline{P}_t^{\text{opt}}$. In fact, setting $A = \mathbf{0}$ still permits to infer frequency regulation following the argumentation of Theorem 1. ◇

Remark 12 (Region of Attraction): LaSalle's invariance principle can be applied to all bounded solutions. As follows from Lemma 2, we have that on the sliding manifold the considered incremental storage function attains a local minimum at the desired steady state, which allows us to show the existence of a region of attraction once the system evolves on the sliding manifold. Furthermore, the time to converge to the sliding manifold can be made arbitrarily small by properly initialing the system and choosing the gains of the SSOSM control algorithm. To characterize the region of attraction requires a careful analysis of the level sets associated with the incremental storage function $\mathcal{S}$, as well as of the trajectories outside of the sliding manifold. A preliminary (numerical) assessment indicates that the region of attraction is large, but a thorough analysis is left as a future endeavor. ◇

Remark 13 (Stability of Primal-Dual-Based Approaches): To accommodate the additional dynamics of states υ and λ appearing in primal-dual-based augmented system (30), an additional storage term is required in Lemma 6, namely

$$\mathcal{S}_3 = \frac{1}{2}(\upsilon - \overline{\upsilon})^T(\upsilon - \overline{\upsilon}) + \frac{1}{2}(\lambda - \overline{\lambda})^T(\lambda - \overline{\lambda}) \tag{37}$$

where $\overline{\upsilon}$ and $\overline{\lambda}$ satisfy the steady-state equations

$$\begin{aligned} \mathbf{0} &= -\overline{\theta} + \overline{P}_t^{\text{opt}} - M_1(M_2 + M_3)^{-1}(\nabla C(\overline{\theta}) - \overline{\lambda}) \\ \mathbf{0} &= -\mathcal{B}^T\overline{\lambda} \\ \mathbf{0} &= \mathcal{B}\overline{\upsilon} - \overline{\theta} + P_d. \end{aligned} \tag{38}$$

Consequently, $\mathcal{S}_2 + \mathcal{S}_3$ satisfies along the solutions to the system, constrained to the manifold $\sigma = \dot{\sigma} = \mathbf{0}$

$$\begin{aligned} \dot{\mathcal{S}}_2 + \dot{\mathcal{S}}_3 = &-(P_t - \theta)^T M_1^{-1}(M_2 + M_3)(P_t - \theta) \\ &-(\theta - \overline{\theta})^T(\nabla C(\theta) - \nabla C(\overline{\theta})) \\ &-\left(P_t - \overline{P}_t^{\text{opt}}\right)^T(f - \mathbf{0}). \end{aligned}$$

Note that, as a result of the mean value theorem, $-(\theta - \overline{\theta})^T(\nabla C(\theta) - \nabla C(\overline{\theta})) = -(\theta - \overline{\theta})^T\nabla^2 C(\tilde{\theta})(\theta - \overline{\theta}) \leq 0$, for some $\tilde{\theta}_i \in [\theta_i, \overline{\theta}_i]$, for all $i \in \mathcal{V}$. The matrix $\nabla^2 C(\tilde{\theta}) \in \mathbb{R}^{n \times n}$ is a positive definite due to the strict convexity of $C(\cdot)$. The proof of Theorem 1 can now be repeated using the incremental storage function $\mathcal{S} = \mathcal{S}_1 + \mathcal{S}_2 + \mathcal{S}_3$. ◇

VI. Case Study

In this section, the proposed control solution is assessed in simulation, by implementing a power network partitioned into four areas.[6] Three different scenarios are investigated and the topology of the considered power network is represented in Fig. 3, together with the communication network (dashed lines).

The line parameters are $B_{12} = -5.4$ p.u., $B_{23} = -5.0$ p.u., $B_{34} = -4.5$ p.u., and $B_{14} = -5.2$ p.u., while the network parameters and the power demand ΔP_{di} of each area are provided in Table II, where a base power of 1000 MW is assumed. The matrices in (18) are chosen as $M_1 = \text{diag}(3.4, 2.7, 3.0, 3.2)$, $M_2 = \text{diag}(1, 1.1, 1.2, 0.9)$, $M_3 = \text{diag}(0.10, 0.09, 0.08, 0.11)$, and $M_4 = -(M_2 + M_3)$, while the control amplitude $W_{\max_i}$ and the parameter α_i^*, in (26) are equal to 10 and 1, respectively, for all $i \in \mathcal{V}$. Note that any other choice of $M_1, \ldots, M_4$, as defined in (18), is admissible.

A. Scenario 1: Power Demand Variation

The system is initially at the steady state. Then, at the time instant $t = 1$ s, the power demand in each area is increased according to the values reported in Table II. From Fig. 10, one can observe that the frequency deviations converge asymptotically to zero after a transient where the frequency drops because of the increasing load, while the

[6] See [55] on how the IEEE New England 39-bus system can be represented by a network consisting of four areas.

TABLE II
NOMINAL NETWORK PARAMETERS AND POWER DEMAND

		Area 1	Area 2	Area 3	Area 4
T_{pi}	(s)	21.0	25.0	23.0	22.0
T_{ti}	(s)	0.30	0.33	0.35	0.28
T_{gi}	(s)	0.080	0.072	0.070	0.081
T_{Vi}	(s)	5.54	7.41	6.11	6.22
K_{pi}	(s^{-1} p.u.$^{-1}$)	120.0	112.5	115.0	118.5
R_i	(s^{-1} p.u.$^{-1}$)	2.5	2.7	2.6	2.8
X_{di}	(p.u.)	1.85	1.84	1.86	1.83
X'_{di}	(p.u.)	0.25	0.24	0.26	0.23
$\overline{E}_{fi}$	(p.u.)	1.0	1.0	1.0	1.0
B_{ii}	(p.u.)	−13.6	−12.9	−12.3	−12.3
$T_{\theta i}$	(s)	0.33	0.33	0.33	0.33
$\mathcal{Q}_i$	(10^4 \$ h^{-1})	2.42	3.78	3.31	2.75
$\mathcal{R}_i$	(10^4 \$ h^{-1})	0.11	0.10	0.13	0.12
$\mathcal{C}_i$	(10^4 \$ h^{-1})	0.91	1.74	1.32	1.05
$P_{di}(0)$	(p.u.)	0.010	0.015	0.012	0.014
ΔP_{di}	(p.u.)	0.010	0.015	0.012	0.014

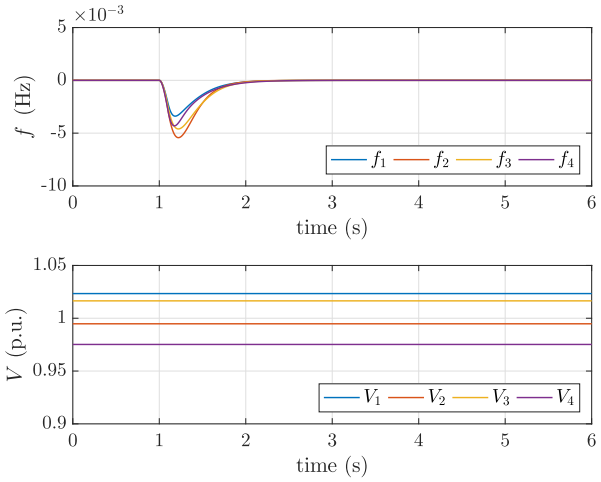

Fig. 4. Scenario 1. Time evolution of the frequency deviations and voltage dynamics, considering a power demand variation at the time instant $t = 1$ s.

voltages remain constant. Indeed, one can note from Fig. 11 that the proposed controllers increase the power generation in order to reach again a zero steady-state frequency deviation. Moreover, the total power demand is (optimally) shared among the areas, and the steady-state marginal costs are identical, minimizing the total generation costs. Finally, Fig. 12 shows the power flows through the power network and the sliding functions.

B. Scenario 2: Opening of a Line

The system is initially at the steady state. Then, at the time instant $t = 1$ s, the line interconnecting Area 1 and Area 4 is opened. From Fig. 7, one can observe that the frequency deviations converge asymptotically to zero after a transient where the frequency varies because of the opening of the line, while the voltages remain constant. Indeed, one can note from Fig. 8 that the proposed controllers regulate

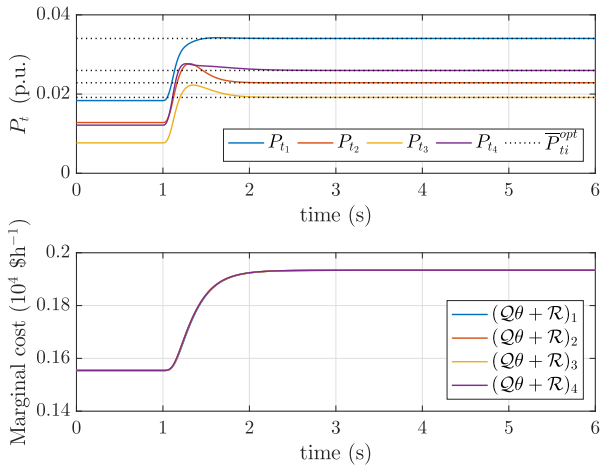

Fig. 5. Scenario 1. Time evolution of the turbine output powers and marginal costs, considering a power demand variation at the time instant $t = 1$ s.

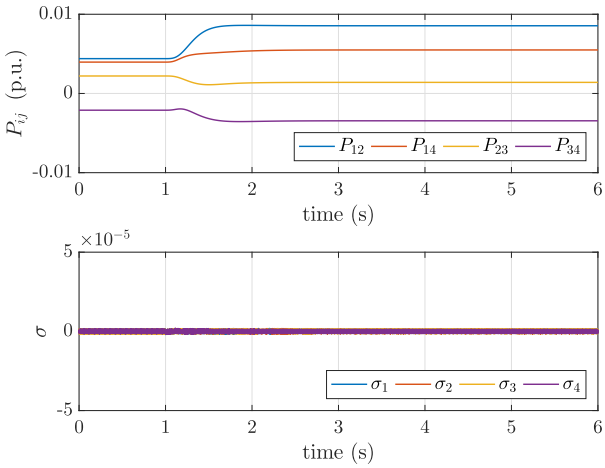

Fig. 6. Scenario 1. Time evolution of the power flows and sliding functions, considering a power demand variation at the time instant $t = 1$ s.

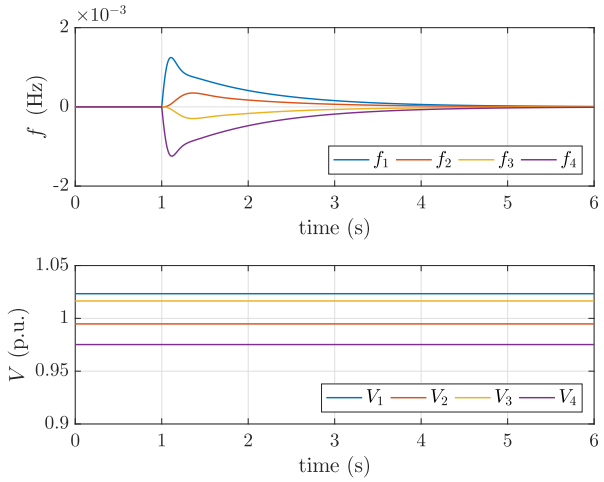

Fig. 7. Scenario 2. Time evolution of the frequency deviations and voltage dynamics, considering the opening of the line {1,4} at the time instant $t = 1$ s.

the power generation in order to reach again a zero steady-state frequency deviation. Moreover, the total power demand is still (optimally) shared among the areas, and the steady-state

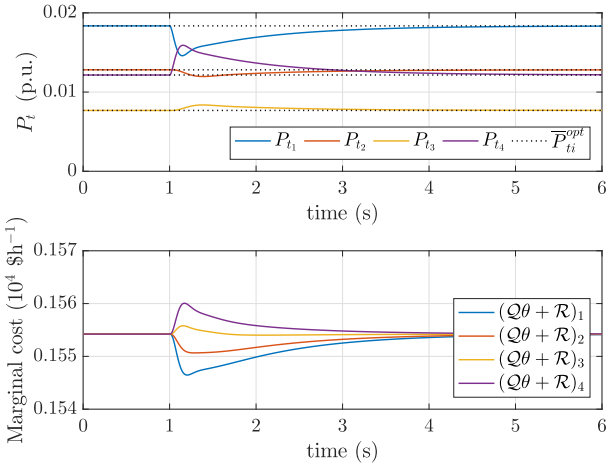

Fig. 8. Scenario 2. Time evolution of the turbine output powers and marginal costs, considering the opening of the line {1,4} at the time instant $t = 1$ s.

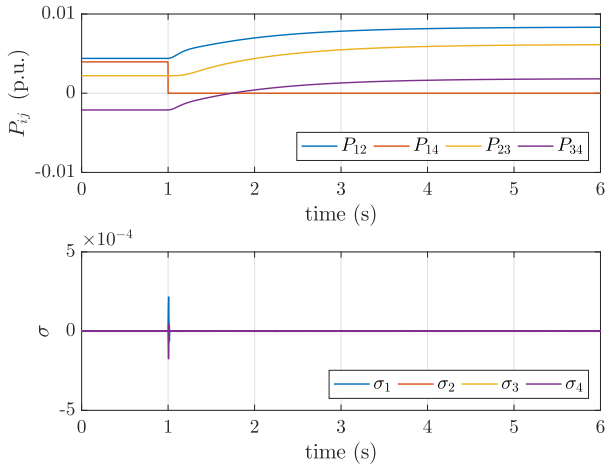

Fig. 9. Scenario 2. Time evolution of the power flows and sliding functions, considering the opening of the line {1,4} at the time instant $t = 1$ s.

marginal costs are identical, minimizing the total generation costs. Finally, Fig. 9 shows the power flows through the power network and the sliding functions.

C. Scenario 3: Failing of a Communication Link

The system is initially at the steady state. Then, at the time instant $t = 0.5$ s the communication link between Area 1 and Area 2 fails, while at the time instant $t = 1$ s, the power demand in each area is increased according to the values reported in Table II. From Fig. 10, one can observe that the frequency deviations converge asymptotically to zero after a transient where the frequency drops because of the increasing load, while the voltages remain constant. Indeed, one can note from Fig. 11 that the proposed controllers increase the power generation in order to reach again a zero steady-state frequency deviation. However, the total power demand is nonoptimally shared among the areas, and only the steady-state marginal costs of Area 2, Area 3, and Area 4 are identical. This is due to the failing of the communication link, which prevents Area 1 from communicating with the other Areas.

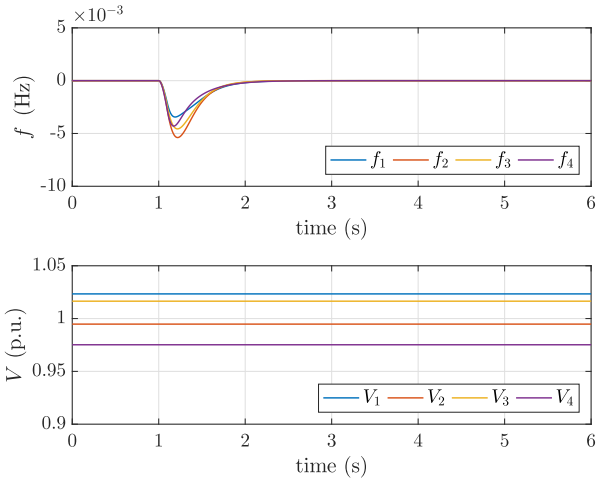

Fig. 10. Scenario 3. Time evolution of the frequency deviations and voltage dynamics, considering the failing of the communication link {1,2} at the time instant $t = 0.5$ s, and a power demand variation at the time instant $t = 1$ s.

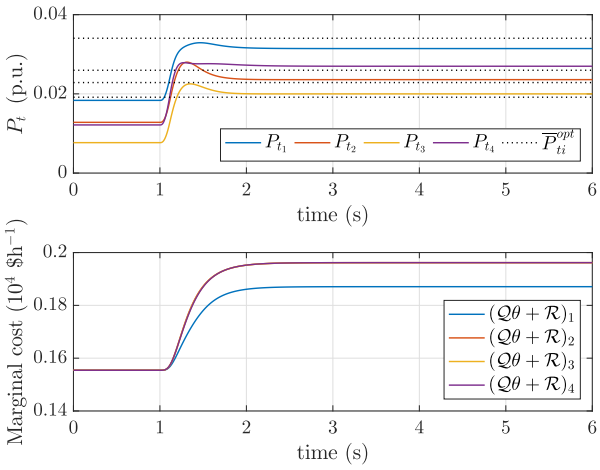

Fig. 11. Scenario 3. Time evolution of the turbine output powers and marginal costs, considering the failing of the communication link {1,2} at the time instant $t = 0.5$ s, and a power demand variation at the time instant $t = 1$ s.

Finally, Fig. 12 shows the power flows through the power network and the sliding functions.

D. Comparison With [41]

In this Section, the proposed control scheme is compared with the controlled proposed in [41], which is given as

$$\begin{aligned} T_\theta \dot{\theta} &= -\theta + P_g - (\mathbb{I}_4 - R^{-1}) f - \mathcal{Q}\mathcal{L}^{\text{com}}(\mathcal{Q}\theta + \mathcal{R}) \\ u &= \theta \end{aligned} \tag{39}$$

where we take $T_\theta = \mathbb{I}_4$. We refer to [41] for the details. Here, we repeat Scenario 1 with the distributed controller (39). The resulting frequency deviations and turbine output powers are provided in Fig. 13. In comparison with the proposed control scheme in this paper (see Figs. 4 and 5), one can notice that the overall response when controller (39) is used, is slightly slower, with a larger frequency drop. On the other hand, the turbine output powers do not experience the overshoot

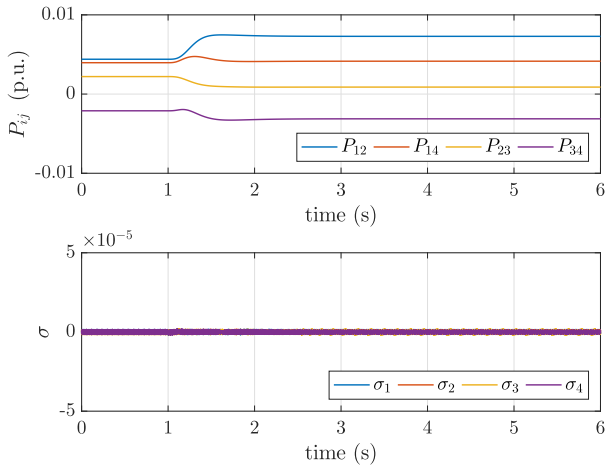

Fig. 12. Scenario 3. Time evolution of the power flows and sliding functions, considering the failing of the communication link {1,2} at the time instant $t = 0.5$ s, and a power demand variation at the time instant $t = 1$ s.

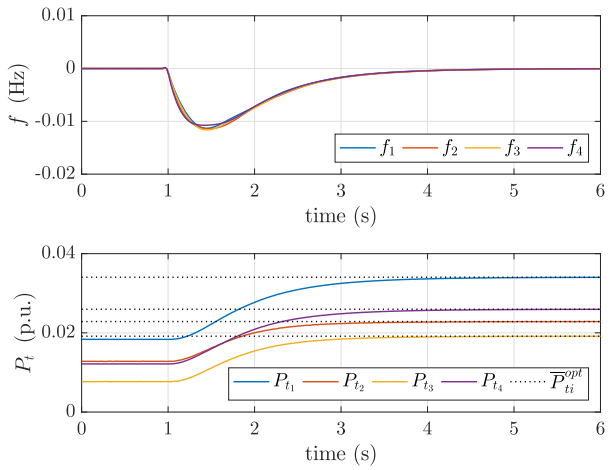

Fig. 13. Scenario 1 with controller (39). Time evolution of the frequency deviations and turbine output powers, considering a power demand variation at the time instant $t = 1$ s.

that can be observed in Fig. 5 for the control scheme that is proposed in this paper.

VII. Conclusion

A D-SSOSM control scheme is proposed to solve an OLFC problem in power systems. In this paper, we adopted a nonlinear model of a power network, including voltage dynamics, where each node is represented by an (equivalent) generator including second-order turbine-governor dynamics. Based on a suitable chosen sliding manifold, the controlled turbine-governor system, constrained to this manifold, possesses an incremental passivity property that is exploited to prove that the frequency deviation asymptotically approaches zero and an economic dispatch is achieved. Designing the SMs, based on passivity considerations, appears to be powerful and we will pursue this approach within different settings, such as achieving power sharing in microgrids. In addition, we would like to compare the performance of the proposed SM-based control scheme in greater detail with other approaches to OLFC appearing in the literature. Since the underlying communication network plays a critical role for the distributed controller, future research directions should also focus on possible delays, discrete time communication, optimal topologies, and larger classes of directed networks.

Appendix

A. Incremental Passivity of the Power Network

Incremental passivity has been shown to play an outstanding role in the analysis of power networks and related controller designs. Particularly, for system (5) a useful passivity property has been established before in [26], and we recall some essential results for the sake of completeness. To facilitate the discussion, we first define "incremental passivity."

Definition 1 (Incremental Passivity): System

$$\begin{aligned} \dot{x} &= \zeta(x, u) \\ y &= h(x) \end{aligned} \tag{40}$$

$x \in \mathbb{R}^n$, $u, y \in \mathbb{R}^m$, is incrementally passive with respect to[7] a constant triplet $(\overline{x}, \overline{u}, \overline{y})$ satisfying

$$\begin{aligned} \mathbf{0} &= \zeta(\overline{x}, \overline{u}) \\ \overline{y} &= h(\overline{x}) \end{aligned} \tag{41}$$

if there exists a continuously differentiable function $\mathcal{S} : \mathbb{R}^n \to \mathbb{R}_+$, such that for all $x \in \mathbb{R}^n$, $u \in \mathbb{R}^m$ and $y = h(x)$, $\overline{y} = h(\overline{x})$

$$\dot{\mathcal{S}} = \frac{\partial \mathcal{S}}{\partial x}\zeta(x, u) + \frac{\partial \mathcal{S}}{\partial \overline{x}}\zeta(\overline{x}, \overline{u}) \leq -W(y, \overline{y}) + (y - \overline{y})^T(u - \overline{u}). \tag{42}$$

In case $W(y, \overline{y}) > 0$, the system is called "*output strictly* incrementally passive." In case $\mathcal{S}$ is not lower bounded, the system is called "incrementally *cyclo*-passive." ◇

To state an incremental passivity property of (5), we make use of the following storage function [26], [56]:

$$S_1(\eta, f, V) = \frac{1}{2} f^T T_p f + \frac{1}{2} V^T E(\eta) V \tag{43}$$

that can also be interpreted as a Hamiltonian function of the system [15].

Lemma 5 (Incremental Cyclo-Passivity of (5)): System (5) with input P_t and output f is an output strictly incrementally cyclo-passive system, with respect to the constant $(\overline{\eta}, \overline{f}, \overline{V})$ satisfying (8).

Proof: For notational convenience, we define $x = (\eta, f, V)$. A tedious but straightforward evaluation of (note the use of a calligraphic $\mathcal{S}$)

$$\mathcal{S}_1(x) = S_1(x) - S_1(\overline{x}) - \nabla S_1(\overline{x})^T(x - \overline{x}) \tag{44}$$

shows that $\mathcal{S}_1(x)$ satisfies [26], [56]

$$\begin{aligned} \dot{\mathcal{S}}_1(x) = -(f - \overline{f})^T K_p^{-1}(f - \overline{f}) - \dot{V}^T T_V (X_d - X_d')^{-1} \dot{V} \\ + (f - \overline{f})^T (P_t - \overline{P}_t) \end{aligned} \tag{45}$$

along the solutions to (5). ■

[7]We state the incremental passivity property with respect to a steady state solution, and not with respect to any solution.

For the stability analysis in Section V, the following technical assumption is needed on the steady state that eventually allows us to infer boundedness of solutions.[8]

Assumption 5 (Steady-State Voltages and Voltage Angles): Let $\overline{V} \in \mathbb{R}^n_{>0}$ and let differences in steady-state voltage angles satisfy

$$\overline{\eta}_k \in \left(-\frac{\pi}{2}, \frac{\pi}{2}\right) \quad \forall\, k \in \mathcal{E}. \tag{46}$$

Furthermore, for all $i \in \mathcal{V}$ it holds that

$$\frac{1}{X_{di} - X'_{di}} - B_{ii} + \sum_{k\sim\{i,j\}\in\mathcal{E}} \frac{B_{ij}(\overline{V}_i + \overline{V}_j \sin^2(\overline{\eta}_k))}{\overline{V}_i \cos(\overline{\eta}_k)} > 0. \tag{47}$$

◇

The assumption above holds if the generator reactances are small compared to the line reactances and the differences in voltage (angles) are small [56]. It is important to note that this holds for typical operation points of the power network. The main consequence of Assumption 5 is that the incremental storage function $\mathcal{S}_1$ now obtains a strict local minimum at a steady state satisfying (8).

Lemma 6 (Local Minimum of $\mathcal{S}_1$): Let Assumption 3 hold. Then, the incremental storage function $\mathcal{S}_1$ has a local minimum at $(\overline{\eta}, \overline{f}, \overline{V})$ satisfying (8).

Proof: Under Assumption 5, the Hessian of (43), evaluated at $(\overline{\eta}, \overline{f}, \overline{V})$, is positive definite [26, Lemma 2], [56, Proposition 1]. Consequently, S_1 is strictly convex around $(\overline{\eta}, \overline{f}, \overline{V})$. The incremental storage function (44) is defined as a Bregman distance [57] associated with (43) for the points (η, f, V) and $(\overline{\eta}, \overline{f}, \overline{V})$. Due to the strict convexity of S_1 around $(\overline{\eta}, \overline{f}, \overline{V})$, (44) has a local minimum at $(\overline{\eta}, \overline{f}, \overline{V})$. ■

B. Sliding Mode Control

In this section, we recall some definitions that are essential to SM control. To this end, we consider system

$$\dot{x} = \zeta(x, u) \tag{48}$$

with $x \in \mathbb{R}^n$, $u \in \mathbb{R}^m$.

Definition 2 (Sliding Function): The sliding function $\sigma(x) : \mathbb{R}^n \to \mathbb{R}^m$ is a sufficiently smooth output function of system (48). ◇

Definition 3 (r-Sliding Manifold): The r-sliding manifold[9] is given as

$$\left\{x \in \mathbb{R}^n, u \in \mathbb{R}^m : \sigma = L_\zeta \sigma = \cdots = L_\zeta^{(r-1)} \sigma = \mathbf{0}\right\} \tag{49}$$

where $L_\zeta^{(r-1)}\sigma(x)$ is the $(r-1)$th order Lie derivative of $\sigma(x)$ along the vector field $\zeta(x, u)$. With a slight abuse of notation, we also write $L_\zeta \sigma(x) = \dot{\sigma}(x)$. ◇

Definition 4 (r-SM): An r-order SM is enforced from $t = T_r \geq 0$, when, starting from an initial condition $x(0) = x_0$, the state of (48) reaches the r–sliding manifold (49), and remains there for all $t \geq T_r$. ◇

[8]In case boundedness of solutions can be inferred by other means, Assumption 5 can be omitted.

[9]For the sake of simplicity, the order r of the sliding manifold is omitted in the following.

Furthermore, the order of a SM controller is identical to the order of the SM that it is aimed at enforcing.

REFERENCES

[1] M. Cucuzzella, S. Trip, C. De Persis, and A. Ferrara, "Distributed second order sliding modes for optimal load frequency control," in *Proc. Amer. Control Conf. (ACC)*, Seattle, WA, USA, 2017, pp. 3451–3456.

[2] D. Apostolopoulou, A. D. Domínguez-García, and P. W. Sauer, "An assessment of the impact of uncertainty on automatic generation control systems," *IEEE Trans. Power Syst.*, vol. 31, no. 4, pp. 2657–2665, Jul. 2016.

[3] A. M. Ersdal, L. Imsland, and K. Uhlen, "Model predictive load-frequency control," *IEEE Trans. Power Syst.*, vol. 31, no. 1, pp. 777–785, Jan. 2016.

[4] M. Zribi, M. Al-Rashed, and M. Alrifai, "Adaptive decentralized load frequency control of multi-area power systems," *Int. J. Elect. Power Energy Syst.*, vol. 27, no. 8, pp. 575–583, 2005.

[5] C. Chang and W. Fu, "Area load frequency control using fuzzy gain scheduling of pi controllers," *Electr. Power Syst. Res.*, vol. 42, no. 2, pp. 145–152, 1997.

[6] S. Trip, M. Cucuzzella, A. Ferrara, and C. De Persis, "An energy function based design of second order sliding modes for automatic generation control," in *Proc. 20th IFAC World Congr.*, Toulouse, France, Jul. 2017, pp. 11613–11618.

[7] Y. G. Rebours, D. S. Kirschen, M. Trotignon, and S. Rossignol, "A survey of frequency and voltage control ancillary services—Part I: Technical features," *IEEE Trans. Power Syst.*, vol. 22, no. 1, pp. 350–357, Feb. 2007.

[8] L. L. Lai, *Power System Restructuring and Deregulation: Trading, Performance and Information Technology*. Hoboken, NJ, USA: Wiley, 2001.

[9] D. K. Molzahn *et al.*, "A survey of distributed optimization and control algorithms for electric power systems," *IEEE Trans. Smart Grid*, vol. 8, no. 6, pp. 2941–2962, Nov. 2017.

[10] S. Trip and C. De Persis, "Communication requirements in a master-slave control structure for optimal load frequency control," in *Proc. IFAC World Congr.*, Toulouse, France, 2017, pp. 10519–10524.

[11] F. Dörfler and S. Grammatico, "Gather-and-broadcast frequency control in power systems," *Automatica*, vol. 79, pp. 296–305, May 2017.

[12] K. Xi, J. L. A. Dubbeldam, H. X. Lin, and J. H. van Schuppen. (Sep. 2017). "Power-imbalance allocation control of power systems-secondary frequency control." [Online]. Available: https://arxiv.org/abs/1703.02855

[13] X. Zhang and A. Papachristodoulou, "A real-time control framework for smart power networks: Design methodology and stability," *Automatica*, vol. 58, pp. 43–50, Aug. 2015.

[14] N. Li, C. Zhao, and L. Chen, "Connecting automatic generation control and economic dispatch from an optimization view," *IEEE Trans. Control Netw. Syst.*, vol. 3, no. 3, pp. 254–264, Sep. 2016.

[15] T. Stegink, C. De Persis, and A. van der Schaft, "A unifying energy-based approach to stability of power grids with market dynamics," *IEEE Trans. Autom. Control*, vol. 62, no. 6, pp. 2612–2622, Jun. 2017.

[16] S. You and L. Chen, "Reverse and forward engineering of frequency control in power networks," in *Proc. 53rd IEEE Conf. Decis. Control*, Los Angeles, CA, USA, Dec. 2014, pp. 191–198.

[17] A. Kasis, E. Devane, C. Spanias, and I. Lestas, "Primary frequency regulation with load-side participation—Part I: Stability and optimality," *IEEE Trans. Power Syst.*, vol. 32, no. 5, pp. 3505–3518, Sep. 2017.

[18] A. Jokić, M. Lazar, and P. P. J. van den Bosch, "Real-time control of power systems using nodal prices," *Int. J. Elect. Power Energy Syst.*, vol. 31, no. 9, pp. 522–530, 2009.

[19] R. Mudumbai, S. Dasgupta, and B. B. Cho, "Distributed control for optimal economic dispatch of a network of heterogeneous power generators," *IEEE Trans. Power Syst.*, vol. 27, no. 4, pp. 1750–1760, Nov. 2012.

[20] Z. Miao and L. Fan, "Achieving economic operation and secondary frequency regulation simultaneously through local feedback control," *IEEE Trans. Power Syst.*, vol. 32, no. 1, pp. 85–93, Jan. 2017.

[21] D. Cai, E. Mallada, and A. Wierman, "Distributed optimization decomposition for joint economic dispatch and frequency regulation," in *Proc. 54th IEEE Conf. Decis. Control (CDC)*, Dec. 2015, pp. 15–22.

[22] D. Apostolopoulou, P. W. Sauer, and A. D. Domínguez-García, "Distributed optimal load frequency control and balancing authority area coordination," in *Proc. North Amer. Power Symp. (NAPS)*, 2015, Oct. 2015, pp. 1–5.

[23] P. Yi, Y. Hong, and F. Liu, "Distributed gradient algorithm for constrained optimization with application to load sharing in power systems," *Syst. Control Lett.*, vol. 83, no. 9, pp. 45–52, 2015.
[24] P. Yi, Y. Hong, and F. Liu, "Initialization-free distributed algorithms for optimal resource allocation with feasibility constraints and application to economic dispatch of power systems," *Automatica*, vol. 74, pp. 259–269, Dec. 2016.
[25] M. Bürger, C. De Persis, and S. Trip, "An internal model approach to frequency regulation in inverter-based microgrids with time-varying voltages," in *Proc. IEEE 53rd Annu. Conf. Decis. Control (CDC)*, Groningen, The Netherlands, Dec. 2014, pp. 223–228.
[26] S. Trip, M. Bürger, and C. De Persis, "An internal model approach to (optimal) frequency regulation in power grids with time-varying voltages," *Automatica*, vol. 64, pp. 240–253, Feb. 2016.
[27] J. Schiffer and F. Dörfler, "On stability of a distributed averaging PI frequency and active power controlled differential-algebraic power system model," in *Proc. Eur. Control Conf. (ACC)*, 2016, pp. 1487–1492.
[28] C. Zhao, E. Mallada, and F. Dörfler, "Distributed frequency control for stability and economic dispatch in power networks," in *Proc. Amer. Control Conf. (ACC)*, Jul. 2015, pp. 2359–2364.
[29] K. Xi, H. X. Lin, C. Shen, and J. H. van Schuppen. (Dec. 2017). "Multi-level power-imbalance allocation control for secondary frequency control in power systems." [Online]. Available: https://arxiv.org/abs/1708.03832
[30] N. Monshizadeh, C. De Persis, A. J. van der Schaft, and J. M. A. Scherpen. (Sep. 2016). "A novel reduced model for electrical networks with constant power loads." [Online]. Available: https://arxiv.org/abs/1512.08250
[31] M. Andreasson, D. V. Dimarogonas, K. H. Johansson, and H. Sandberg, "Distributed vs. centralized power systems frequency control," in *Proc. Eur. Control Conf. (ECC)*, Jul. 2013, pp. 3524–3529.
[32] S. Kar and G. Hug, "Distributed robust economic dispatch in power systems: A consensus + innovations approach," in *Proc. IEEE Power Energy Soc. Gen. Meeting*, Jul. 2012, pp. 1–8.
[33] G. Binetti, A. Davoudi, F. L. Lewis, D. Naso, and B. Turchiano, "Distributed consensus-based economic dispatch with transmission losses," *IEEE Trans. Power Syst.*, vol. 29, no. 4, pp. 1711–1720, Jul. 2014.
[34] N. Rahbari-Asr, U. Ojha, Z. Zhang, and M. Chow, "Incremental welfare consensus algorithm for cooperative distributed generation/demand response in smart grid," *IEEE Trans. Smart Grid*, vol. 5, no. 6, pp. 2836–2845, Nov. 2014.
[35] S. Yang, S. Tan, and J.-X. Xu, "Consensus based approach for economic dispatch problem in a smart grid," *IEEE Trans. Power Syst.*, vol. 28, no. 4, pp. 4416–4426, Nov. 2013.
[36] T. Yang, D. Wu, Y. Sun, and J. Lian, "Minimum-time consensus-based approach for power system applications," *IEEE Trans. Ind. Electron.*, vol. 63, no. 2, pp. 1318–1328, Feb. 2016.
[37] Z. Zhang and M.-Y. Chow, "Convergence analysis of the incremental cost consensus algorithm under different communication network topologies in a smart grid," *IEEE Trans. Power Syst.*, vol. 27, no. 4, pp. 1761–1768, Nov. 2012.
[38] K. Vrdoljak, N. Perić, and I. Petrović, "Sliding mode based load-frequency control in power systems," *Elect. Power Syst. Res.*, vol. 80, no. 5, pp. 514–527, 2010.
[39] Y. Mi, Y. Fu, D. Li, C. Wang, P. C. Loh, and P. Wang, "The sliding mode load frequency control for hybrid power system based on disturbance observer," *Int. J. Elect. Power Energy Syst.*, vol. 74, pp. 446–452, Jan. 2016.
[40] G. Bartolini, A. Ferrara, and E. Usai, "Chattering avoidance by second-order sliding mode control," *IEEE Trans. Autom. Control*, vol. 43, no. 2, pp. 241–246, Feb. 1998.
[41] S. Trip and C. De Persis, "Distributed optimal load frequency control with non-passive dynamics," *IEEE Trans. Control Netw. Syst.*, p. 1, 2017, doi: 10.1109/TCNS.2017.2698259.
[42] A. Kasis, N. Monshizadeh, E. Devane, and I. Lestas. (Mar. 2017). "Stability and optimality of distributed secondary frequency control schemes in power networks." [Online]. Available: https://arxiv.org/abs/1703.00532
[43] J. Machowski, J. Bialek, and D. J. Bumby, *Power System Dynamics: Stability and Control*, 2nd ed. Hoboken, NJ, USA: Wiley, 2008.
[44] P. Kundur, N. J. Balu, and M. G. Lauby, *Power System Stability and Control*, vol. 7. New York, NY, USA: McGraw-Hill 1994.
[45] T. Stegink, C. De Persis, and A. van der Schaft. (Mar. 2016). "Optimal power dispatch in networks of high-dimensional models of synchronous machines." [Online]. Available: https://arxiv.org/abs/1603.06688
[46] C.-C. Chu and H.-D. Chiang, "Constructing analytical energy functions for network-preserving power system models," *Circuits, Syst. Signal Process.*, vol. 24, no. 4, pp. 363–383, 2005.
[47] K. R. Padiyar, *Structure Preserving Energy Functions in Power Systems: Theory and Applications*. New York, NY, USA: Taylor & Francis, 2013.
[48] G. Rinaldi, M. Cucuzzella, and A. Ferrara, "Third order sliding mode observer-based approach for distributed optimal load frequency control," *IEEE Control Syst. Lett.*, vol. 1, no. 2, pp. 215–220, Oct. 2017.
[49] V. I. Utkin, *Sliding Modes in Control and Optimization*. New York, NY, USA: Springer-Verlag, 1992.
[50] A. Levant, "Higher-order sliding modes, differentiation and output-feedback control," *Int. J. Control*, vol. 76, nos. 9–10, pp. 924–941, Jan. 2003.
[51] G. Bartolini, A. Ferrara, and E. Usai, "On boundary layer dimension reduction in sliding mode control of SISO uncertain nonlinear systems," in *Proc. IEEE Int. Conf. Control Appl.*, vol. 1, Trieste, Italy, Sep. 1998, pp. 242–247.
[52] G. P. Incremona, M. Cucuzzella, and A. Ferrara, "Adaptive suboptimal second-order sliding mode control for microgrids," *Int. J. Control*, vol. 89, no. 9, pp. 1849–1867, 2016.
[53] A. Levant, "Sliding order and sliding accuracy in sliding mode control," *Int. J. Control*, vol. 58, no. 6, pp. 1247–1263, Dec. 1993.
[54] P. Kundur, "Definition and classification of power system stability IEEE/CIGRE joint task force on stability terms and definitions," *IEEE Trans. Power Syst.*, vol. 19, no. 3, pp. 1387–1401, May 2004.
[55] S. Nabavi and A. Chakrabortty, "Topology identification for dynamic equivalent models of large power system networks," in *Proc. Amer. Control Conf. (ACC)*, Jun. 2013, pp. 1138–1143.
[56] C. De Persis and N. Monshizadeh. (2016). "Bregman storage functions for microgrid control." [Online]. Available: https://arxiv.org/abs/1510.05811
[57] L. M. Bregman, "The relaxation method of finding the common point of convex sets and its application to the solution of problems in convex programming," *USSR Comput. Math. Math. Phys.*, vol. 7, no. 3, pp. 200–217, 1967.

Sebastian Trip received the B.Sc. degree in physics, the M.Sc. degree in energy and environmental sciences, and the Ph.D. degree in systems theory from the University of Groningen, Groningen, The Netherlands, in 2017.

From 2017 to 2018, he was a Post-Doctoral Researcher with the University of Groningen. He is currently a Trainee Patent Attorney with EP & C, Rijswijk, The Netherlands. His current research interests include distributed control and optimization, with applications to energy and cyber-physical systems.

Michele Cucuzzella received the bachelor's degree (Hons.) in industrial engineering and the master's degree (Hons.) in electrical engineering from the University of Pavia, Pavia, Italy, in 2012 and 2014, respectively, and the Ph.D. degree in electronics, computer science and electrical engineering from the University of Pavia, in 2018, under the supervision of Prof. A. Ferrara. He is currently pursuing the Ph.D. degree with the Johann Bernoulli Institute for Mathematics and Computer Science, University of Groningen, Groningen, The Netherlands, under the supervision of Prof. A. van der Schaft.

He is currently a Post-Doctoral Researcher with the University of Groningen, in collaboration with Prof. J. Scherpen. His current research interests include nonlinear control, sliding mode control, and event-triggered control with application to power networks.

Claudio De Persis received the Laurea degree in electronic engineering and the Ph.D. degree in system engineering from the University of Rome La Sapienza, Rome, Italy, in 1996 and 2000, respectively.

He held faculty positions at the Department of Mechanical Automation and Mechatronics, University of Twente, Enschede, The Netherlands, and the Department of Computer, Control, and Management Engineering, University of Rome La Sapienza. He is currently a Professor with the Faculty of Science and Engineering, Engineering and Technology Institute, University of Groningen, Groningen, The Netherlands. His current research interests include control theory, with a focus on dynamical control networks, cyber-physical systems, control and optimization of smart grids.

Dr. Persis is currently an Associate Editor of *Automatica* in 2013 and IEEE CONTROL SYSTEMS LETTERS in 2017.

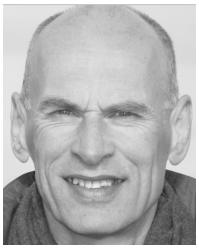

Arjan van der Schaft received the undergraduate and Ph.D. degrees in mathematics from the University of Groningen, Groningen, The Netherlands, in 1979 and 1983, respectively.

In 1982, he joined the Department of Applied Mathematics, University of Twente, Enschede, The Netherlands, where he was appointed as a Full Professor in mathematical systems and control theory in 2000. In 2005, he returned to Groningen as a Full Professor in mathematics. He has co-authored *Variational and Hamiltonian Control Systems* (P.E. Crouch, 1987), *Nonlinear Dynamical Control Systems* (H. Nijmeijer, 1990, 2016), *L2-Gain and Passivity Techniques in Nonlinear Control* (1996, 2000, 2017), *An Introduction to Hybrid Dynamical Systems* (J. M. Schumacher, 2000), and *Port-Hamiltonian Systems: an Introductory Overview* (D. Jeltsema, 2014).

Dr. Schaft is a Fellow of the Institute of Electrical and Electronics Engineersand International Federation of Automatic Control (IFAC). He was a recipient of the 3-yearly awarded Certificate of Excellent Achievements of the IFAC Technical Committee on Nonlinear Systems in 2013. He was an Invited Speaker at the International Congress of Mathematicians, Madrid, 2006.

Antonella Ferrara received the Laurea degree *(magna cum laude)* in electronic engineering and the Ph.D. degree from the University of Genoa, Genoa, Italy, in 1987 and 1992, respectively.

He is currently a Full Professor of automatic control with the University of Pavia, Pavia, Italy. She has authored or co-authored more than 360 papers including 110 journal papers. She has been a coordinator in international and national projects and Associate Editor of several journals. Her current research interests include sliding mode and nonlinear control with application to power systems, robotics, automotive and traffic control.

Dr. Ferrara is a Senior Member of the IEEE Control Systems Society. She was the Chair of the Women in Control Standing Committee, appointed in 2012 and elected member from 2016 to 2018 of the Board of Governors of the IEEE Control Systems Society. She is a Member of the EUCA Council and has been recently appointed ECC Editorial Board Chair. She is currently an Associate Editor of *Automatica*, the *International Journal of Robust and Nonlinear Control*, and IEEE CONTROL SYSTEMS MAGAZINE.